EGR Gas Composition Effects on Ignition Delays in Diesel Combustion

Yoshimitsu Kobashi[1]*, Masaki Todokoro[1], Gen Shibata[1], Hideyuki Ogawa[1],
Toshihiro Mori[2], Daichi Imai[2]

[1] Division of Energy and Environmental Systems, Graduate School of Engineering, Hokkaido University, Japan

[2] Advanced Powertrain Engineering Div. No.1, TOYOTA Motor Corporation, Japan

Abstract

This paper presents the effects on ignition delays of a range of exhaust gas compositions recirculated in the intake air. The ignition delays were measured in a single-cylinder diesel engine introducing a variety of hydrocarbons, nitrogen oxides (NO_x), and carbon monoxide (CO) into the intake gas, and changing the concentrations of these components. The experimental results show that the ignition delay decreases with the NO_x addition, NO_2 promotes the ignition more than NO, and this effect is more pronounced at higher intake gas temperatures. The ignition delay decreases with HC addition under NO_x rich conditions while there is little effect under low NO_x conditions, and the ignition delay changes with the kinds of hydrocarbons. The CO has little effect on the ignition delay. With the aid of chemical reaction analysis, the mechanisms of these changes are elucidated.

* Corresponding author at: Kita 13, Nishi 8, Kita-ku, Sapporo, Hokkaido, Japan
E-mail address: kobashi@eng.hokudai.ac.jp (Y. Kobashi)

Keywords: Ignition Delay, Exhaust Gas Recirculation, Diesel Engine, Nitrogen Oxide

Nomenclature:

$dQ/d\theta$	The rate of the heat release [J/ºCA]
$d^2Q/d\theta^2$	Derivative of the rate of the heat release [J/ºCA/ºCA]
EGR	Exhaust gas recirculation
HCCI	Homogeneous charge compression ignition
IMEP	Indicated mean effective pressure
LTC	Low temperature combustion
LTOR	Low temperature oxidation reaction
PAHs	Polycyclic aromatic hydrocarbons
p_{inj}	Injection pressure [MPa]
TDC	Top dead center
SOI	Start of injection
T_{in}	Intake air temperature [K]
τ_{ign}	Ignition delay [ºCA]

1. Introduction

To respond to increasingly stringent emission and fuel consumption regulations, combustion improvement strategies have been developed for diesel engines. Exhaust gas recirculation (EGR) is an emission control technology enabling significant nitrogen oxides (NO_x) reductions, that are achieved due to the decreased flame temperature attributed to the decreased intake oxygen concentration and increased heat capacity. Further, increases in the EGR rate decreases the flame temperature to a level where no soot is formed [1-3], and lengthens the ignition delay while enhancing the homogeneity

of the gas mixture [4, 5]. Considering the features of these combustion regime termed low temperature combustion (LTC), the potential application of EGR has extended investigations into reductions of soot formation and cooling losses in modern diesel engines [6, 7]. Also, recent research has payed attention to the effects of fuel properties in the LTC since they have significant impacts on the ignition delay and mixture formation that are important factors affecting engine performance and emissions [8-11].

As EGR affects the ignition delays of gas oil significantly, the investigations have been carried out intensively, and have substantiated that the oxygen reduction and thermodynamic effects due to the high specific-heat capacity of carbon dioxide (CO_2) and water (H_2O) lengthen the ignition delays [12-15]. In the LTC regime achieved with a large amount of EGR, however, the intake gas composition would play a more important role in the ignition delays, as the concentrations of unburned hydrocarbons and carbon monoxide (CO) tend to increase in the recirculated intake gas together with the decrease in the oxygen concentration, and as there is also a non-negligible concentration of NO_x that becomes recirculated at high load operation.

In spark-ignition engines, it is known that NO_x enhances the ignition, leading to knocking issues [16]. Sjöberg et al. suggested the possibility that such autoignition was influenced by the presence of unburned or only partially-oxidized hydrocarbons and

68 nitrogen monoxide (NO) in a homogeneous charge compression ignition (HCCI) engine
69 fueled with gasoline and primary reference fuels [17], and Kawasaki et al. demonstrated
70 that the ignition was enhanced with either NO and nitrogen dioxide (NO_2) in a HCCI
71 engine fueled with natural gas [18]. Chemical kinetic studies considering the presence of
72 hydrocarbons and NO_x suggest that the following reaction shows the highest sensitivity
73 to enhancements in the ignition:

74 $$NO + HO_2 = NO_2 + OH \quad \text{(R1)}$$

75 suggesting that this reaction shows a strong dependence on the kind of fuels and that it is
76 important in the low temperature oxidation reaction (LTOR) [19, 20]. This chemical
77 kinetic mechanism may be important for gas oil which is accompanied by large heat
78 release during the LTOR. Using a primary reference fuel with octane number 90, the
79 authors have shown that the ignition of the spray combustion was enhanced by the
80 entrained gas which consists of the intermediate products during the LTOR [21], but less
81 study on the effects of intermediate products on the ignition of gas oil have been
82 implemented as conventional diesel engines primarily have short ignition delays, this is
83 except for some reports which reported that the ambient gases containing methane (CH_4)
84 and propane (C_3H_8) have no facilitating influence on the ignition of the diesel spray [22-
85 25].

The present study proposes to investigate the effects of the EGR gas composition on the ignition delays of diesel combustion in a low temperature combustion regime with low intake oxygen concentrations, particularly focusing on cases where there is both hydrocarbons and NO_x. The ignition delays were measured in a single-cylinder engine while changing the concentrations of hydrocarbons, CO, and NO_x as well as the intake gas temperature. Additional investigation into the effects of the chemical reaction mechanism on the ignition delays were carried out with the CHEMKIN-PRO software [26].

2. Experimental Devices, Setup, and Procedures

2.1 Test Engine and Fuel Used

A four-stroke water-cooled diesel engine (YANMAR, 4TNV98T) was used to measure the ignition delays. This engine was originally composed of four cylinders, and was modified to be a single-cylinder engine by detaching the pistons of three of the cylinders. Table 1 details the specifications of the test engine. The bore and stroke were 98 mm and 110 mm, and the stroke volume was 830 cm^3. A piston with a toroidal bowl geometry was used, and the compression ratio was 17.6. The test engine was equipped with a common-rail fuel injection system. The engine used a G4S injector (DENSO, G4S) equipped with

104 an 8-hole nozzle, nozzle hole diameter 0.125 mm with a spray angle of 155°. A
105 commercially-available gas oil was used as the test fuel.

106 **2.2 Experimental Setup**

107 Figure 1 shows an outline of the experimental setup. The in-cylinder pressure was
108 measured with a piezoelectric pressure sensor (KISTLER, 6125B) for 180 cycles, and the
109 electrical charge was introduced via a charge amplifier (KISTLER, 5011B), converted
110 into a voltage signal, and recorded with a computer via an AD converter (Interface, CBI-
111 320412). This cycle number recorded was limited by the amount of memory of the AD
112 converter, but it was enough in cycle number to obtain representative histories of pressure
113 and heat release rate under the conditions employed in the present study.

114 Unlike the experiments where repetition of measurements is possible, it is difficult for
115 engine tests to repeat many tests at each operating point due to the many data points
116 involved, and in engine test, cycle-by-cycle variations in the combustion process may
117 cause a significant error and deteriorate the accuracy of measurements. In the present
118 study, to mitigate the effects of the cycle-by-cycle variations, the data obtained in the
119 experimental conditions where the coefficient of variance of indicated mean effective
120 pressure were less than 5% were used for the evaluation.

121 The engine employed a low-pressure loop EGR system which contains a diesel

122 oxidation catalyst (DOC) to reduce unburned emissions and a diesel particulate filter
123 (DPF) to remove soot particles. A 5 kW heater was installed into the channel of the intake
124 manifold to control the intake air temperature. The EGR rate was controlled by adjusting
125 the opening positions of two gate valves. One was installed in the EGR channel to control
126 the EGR rate, another was installed in the exhaust channel to maintain a constant exhaust
127 gas pressure equal to the intake air pressure.

128 To simulate the EGR gas composition with pure components, pure gases were
129 introduced into the intake pipe from gas cylinders while controlling the flow rate with
130 mass flow controllers (KOFLOC, Model 3665 for CO and Model 3660 for the other
131 gases) which have accuracy better than ±1.5 and ±1.0% of full scale output (FSO). The
132 flow rates of the pure gases were adjusted to the targeted concentrations at the intake that
133 are calculated with the flow rate of the intake air. The flow rate of the intake air was
134 determined with a differential pressure type flowmeter, and the pressure difference was
135 measured with a digital manometer (Tsukasa Sokken, PE-33-D) which has accuracy
136 better than ±0.5% of FSO. Considering these facts, the impact of the measurement error
137 on the flow rate is negligibly small. Furthermore, the concentrations in the intake gas
138 were measured with the gas analyzer for verification purposes.

139 The intake NO_2 concentration was changed while introducing NO and O_2 into a heated

140 oxidation catalyst.

141 The concentrations of the intake and exhaust gas components were measured with a
142 gas analyzer (Best Sokki, BEX-5100D), with the total hydrocarbons (THC) measured
143 with FID (Flame ionization detector); NO_x with CLD (Chemiluminescence detector); CO
144 and CO_2 with NDIR (Non dispersive infrared); oxygen (O_2) with a dumbbell-type sensor.
145 More detailed measurements of hydrocarbon species in the exhaust gas were carried out
146 with a Fourier transform infrared (FTIR) spectrometer (HORIBA, MEXA-4000FT)
147 which quantifies the concentrations of specified chemical species as detailed in Table 2.
148 A part of the exhaust gas was collected with a sampling bag, and introduced into the FTIR
149 spectrometer after diluting the exhaust gas collected with nitrogen (N_2) to an appropriate
150 concentration.

151 **2.3 Definitions of the Ignition and Start of Injection**

152 The definitions of the ignition and start of injection are shown in Fig.2. The ignition
153 timing was determined as the derivative of the heat release rate $d^2Q/d\theta^2$ where it exceeds
154 5 J/°CA/°CA, and the fuel injection timing was adjusted to fix the ignition timing at -
155 3°CA ATDC. The fuel injection timing was determined as the timing of the drop in the
156 fuel pressure measured with the G4S injector.

157

158 ## 3. Results and Discussion

159 ### 3.1 Nitrogen Oxide Addition under Real EGR Conditions

160 #### 3.1.1 Experimental Conditions

161 The experimental conditions are detailed in Table 3. The injection quantity was fixed
162 at 20 mm^3/cycle. With this fuel quantity, the indicated mean effective pressure (IMEP)
163 was around 0.25 MPa. A naturally aspirated operation was implemented without any
164 boosting, while the oxygen concentration was reduced to 7% with the EGR to ensure low
165 temperature combustion. The intake air temperature was changed to examine the
166 dependence of the ignition delay on the in-cylinder gas temperature.

167 Prior to the ignition delay measurements, the composition of the intake gas was
168 measured. As a result, the concentrations of CO, CO_2, and NO_x were 4%, 7%, and 0 ppm,
169 and those of the hydrocarbons are as shown in Fig.3. The unknown hydrocarbons which
170 are the difference between the THC measured with the FID (BEX-5100D) and the
171 hydrocarbons measured with the FTIR spectrometer (MEXA-4000FT) were
172 approximately half. One major reason for this discrepancy is that the detectable species
173 of the FTIR spectrometer are limited as listed in Table 2. And the FTIR spectroscopy was
174 carried out after the gas was collected with a sampling bag at room temperature so that
175 high boiling point components could not be detected, while the BEX-5100D gas analyzer

176 sucked the gas in via a hot hose maintained at the temperature of 191°C. Except for
177 unknown species, the highest concentration of hydrocarbons was CH_4, followed by C_2H_4,
178 and C_6H_6. Small amounts of C_3H_6, 1,3-C_4H_6 and iso-C_4H_8 were also detected.

179 In this section, NO_x which was not present in the intake gas was supplied from gas
180 cylinders together with the EGR while changing the intake air temperature T_{in}. The intake
181 NO_x concentration changed more widely than can be anticipated in practical diesel
182 engines, to more fully understand details of the dependence on the experimental
183 parameters. The addition of the gases to the intake flow had no direct impact on the EGR
184 rate set to maintain the constant oxygen concentration due to the very low concentrations.

185 **3.1.2 Effects of Nitrogen Oxide Addition on Ignition**

186 Figure 4 shows the changes of the ignition delays with the NO_x concentrations. The
187 open symbols are the case where pure NO was introduced into the intake gas, while the
188 closed symbols are for where a NO and NO_2 mixture produced from NO via the heated
189 oxidation catalyst is introduced into the intake air. The volume fractions of NO and NO_2
190 are detailed in Table 4. Approximately half of NO was converted into NO_2 via the
191 oxidation catalyst.

192 The ignition delay decreased with increasing intake NO concentration, and it
193 decreased significantly with lower concentrations of NO at the higher intake temperature

194 T_{in}. At the lower temperature, reactions R2 and R3 have an inhibiting impact on the
195 ignition vis-a-vis reaction R1, as follows [20, 27]:

196 $$RO_2 + NO = RO + NO_2 \quad \text{(R2)}$$

197 $$NO + OH\ (+M) = HONO\ (+M) \quad \text{(R3)}$$

198 Where R is an alkyl radical. With increasing temperature, reaction R1 becomes more
199 important, and the dissociation of HONO exceeds its production (R3 is reversed),
200 enhancing the ignition.

201 The intake NO_2 has the stronger impact on acceleration of the ignition. A possible
202 explanation is that NO_2 produces reactive radicals in the C_1-C_2 chemistry as follows [16]:

203 $$R' + NO_2 = RO + NO \quad \text{(R4)}$$

204 Where R' is a small alkyl radical. As the intake gas consisted of small hydrocarbons (see
205 Fig.3), this reaction enhanced the oxidation reaction of the in-cylinder gas during the
206 compression stroke, and the ignition of the spray combustion was promoted while
207 entraining the intermediate products into the spray.

208 Figure 5 shows the profiles of the in-cylinder pressure and heat release rate $dQ/d\theta$.
209 The arrows indicating the fuel injection timings were retarded with increases in the NO
210 concentration, to adjust the ignition timing to be at -3°CA ATDC. The heat release before
211 the fuel injection can be seen at the NO concentration of 670 ppm, suggesting that

212 hydrocarbons contained in the in-cylinder gas ignited with the aid of the NO reactions.
213 With the NO concentrations less than 370 ppm, there appeared to be a small heat release
214 before the main heat release. This is a low temperature oxidation reaction (LTOR) of the
215 gas oil as evidenced by the fact that the timing of the heat release is changed with the start
216 of injection (SOI). To compare the LTOR, the heat release rate $dQ/d\theta$ arranged with the
217 crank angle after the SOI is shown in Fig.6. Beginning from 3°CA after SOI, there is a
218 small heat release due to the LTOR. This heat release increased with increases in the NO,
219 suggesting that the intermediate products of the in-cylinder gas facilitated the LTOR.

220 **3.2 Nitrogen Oxide and Hydrocarbon Additions under N_2-dilution Conditions**

221 **3.2.1 Experimental Conditions**

222 The intake gas composition was changed by introducing pure gases from the gas
223 cylinders without use of EGR. The gas compositions investigated for this are detailed in
224 Table 5. The recent paper elucidated that much polycyclic aromatic hydrocarbons (PAHs)
225 are formed in the LTC regime [28], and thus it would be interesting to examine the effects
226 of the PAHs on the ignition. The FTIR spectrometer employed in the present study,
227 however, is not able to detect the PAHs, so that the investigation did not cover the effects
228 of the PAHs on ignition. There is a paper showing that much HCHO is formed and affects
229 ignition delays in the LTC [29], but low concentration of HCHO in the order of tens of

230 ppm was recirculated into the intake according to the FTIR measurement, and HCHO was
231 not introduced in the intake in the present study. The oxygen concentration was set at 11%
232 which is higher than that in the above section, as operation failed due to misfiring at lower
233 oxygen concentrations. In the above section, the passage in the exhaust pipe was narrowed
234 with a valve to recirculate the large amount of the exhaust gas into the intake, causing the
235 increase in the exhaust gas pressure, and in the amount of hot residual gas in the
236 combustion chamber. This might increase the in-cylinder temperature, and shorten the
237 ignition delay. On the other hand, the exhaust valve was fully opened in this section, and
238 less residual gas was remained in the combustion chamber.

239 The CO, NO, and hydrocarbons were introduced on a one-by-one basis to examine
240 their impact on the ignition. To examine the combined effects of NO and hydrocarbons,
241 the CH_4 concentration was fixed at 5000 ppmC, and the hydrocarbon species were
242 changed while increasing the concentrations up to 5000 ppmC. These conditions were
243 determined referring to Fig.3, increasing the concentrations to achieve extreme conditions.
244 The intake air temperature T_{in} was maintained at 125°C, with other conditions the same
245 as in Table 3.

246 **3.2.2 Effects of Nitrogen Oxide and Hydrocarbon Addition on Ignition**

247 Figure 7 shows the ignition delays τ_{ign} with the different intake CO concentrations.

248 The CO concentration had a very small impact on the ignition delay. Figure 8 shows the
249 ignition delays τ_{ign} with the various intake hydrocarbon species and concentrations. There
250 is no significant change in the ignition delays with the addition of the hydrocarbons.

251 Figure 9 shows the ignition delays τ_{ign} with the different intake NO concentrations.
252 The increase in NO decreased the ignition delays, suggesting that NO entrained into the
253 spray enhanced the ignition. The NO concentrations here are rather higher than those
254 under actual EGR conditions, and it is notable that the ignition delay decreases with lower
255 NO concentrations at the higher intake gas temperatures T_{in} (see Fig.4).

256 The profiles of the in-cylinder pressure and heat release rate $dQ/d\theta$ are shown in Fig.10.
257 Similar to Fig.5, there was a small heat release due to the LTOR between the SOI and the
258 main combustion which was promoted with the increase in NO.

259 Figure 11 shows the effects of the hydrocarbon species on the ignition delays τ_{ign}.
260 Compared to the case with only NO, the ignition delays τ_{ign} were decreased with the
261 additions of the other hydrocarbons. This result indicates that the NO and hydrocarbons
262 of the in-cylinder gas reacted and yielded intermediate products that enhance the ignition
263 of the diesel spray. The impact of the C_2H_4 and C_3H_6 additions were equivalent and the
264 strongest, followed by those of the C_3H_8 addition. The addition of CH_4 also decreased the
265 ignition delay but to a smaller degree. The results here were reproducible, and similar

266 tendencies were obtained under the other intake air temperature conditions tested here.

267 **3.2.3 Chemical Kinetic Analysis of the Effects of Nitrogen Oxide and Hydrocarbon**

268 **Additions**

269 The ignition enhancement effects of NO and hydrocarbon addition were analyzed with
270 chemical kinetic calculations. The software used was CHEMKIN-PRO selecting the
271 single-zone IC HCCI Engine model which predicts chemical reactions during a
272 compression and expansion stroke [26]. These calculations were carried out to simulate
273 the chemical reaction of the in-cylinder gas without fuel injections, focusing on the
274 concentration of the OH radical which is known to be the key species in the development
275 of ignition. The development of the reaction model of hydrocarbons and nitrogen oxide
276 species is in progress [30, 31], but the authors chosen the model proposed by Anderlohr
277 et al. [20] since the good agreements on the validations with the experiments in an HCCI
278 engine where the pressure and temperature conditions are relevant to the present study,
279 and the model has been widely utilized in the recent research of internal combustion
280 engines [32, 33].

281 The calculation conditions are equivalent to the engine tests in section 3.2, except for
282 the initial temperature which was adjusted to the calculated temperature close to the TDC
283 (Top dead center) for the engine tests. The concentrations of NO and CH_4 were fixed at

284 100 ppm and 5000 ppmC. The hydrocarbon species of CH_4, C_2H_4, C_3H_6, and C_3H_8 were
285 added to the NO and CH_4 mixture on a one-by-one basis while maintain the
286 concentrations of 5000 ppmC. Note that no gas oil component was fed in the calculation
287 to examine the ignition promotion effects of the NO and hydrocarbon addition.

288 Figure 12 shows the profiles of the temperature and the OH radical, for the mixture of
289 CH_4 (5000 ppmC) and C_2H_4 (5000 ppmC). In this calculation, no high temperature
290 oxidation reaction took place due to the very lean mixture, and the impact on the chemical
291 reactions on the temperature rise was limited in analogy with the experiments shown in
292 the above sections. With the addition of NO, the OH concentration became 500 times that
293 without the addition of NO at the TDC as can be seen in this figure. The effects of the gas
294 composition on the OH concentrations are compared in Fig.13, where four different
295 hydrocarbons at 5000 ppmC are mixed with CH_4 (5000 ppmC) and NO (100 ppm). The
296 highest OH concentration was achieved with the mixture of C_3H_6, followed by that of
297 C_2H_4. The OH concentrations of C_3H_8 and CH_4 were lower than those of C_3H_6 and C_2H_4.
298 The order of the OH concentrations was analogous with that of the ignition delay
299 measured in the engine tests, except for the opposite trend between C_3H_8 and CH_4.

300 To develop an understanding of the chemical reactions that predominantly produced
301 the OH radical, the rate of production was analyzed. Figure 14 shows the major rates of

302 production with respect to the OH radical at the TDC. Regardless of the hydrocarbon
303 species, the OH production was governed with the R1 reaction. The OH production via
304 the R1 reaction was highest with the addition of C_3H_6, followed by that of C_2H_4. The rates
305 of OH production of C_3H_8 and CH_4 were lower than those of C_3H_6 and C_2H_4. Note that
306 the range of the horizontal axis in C_3H_6 is larger than that in the others. At the TDC, the
307 HONO dissociation in R3 as well as the CH_3OO dissociation was pronounced. The OH
308 radical was predominantly consumed by the reactions with CH_4 and the other added
309 hydrocarbons. From this result, it may be summarized that the R1 reaction is most
310 important in the OH production.

311 The rate of production was analyzed with respect to HO_2. The major rates of HO_2
312 production are shown in Fig.15. Note that the range of the horizontal axis in C_3H_6 is larger
313 than that in the others. The reactions relating to the HO_2 production with C_3H_8 and CH_4
314 were similar, except for the fact that the intermediate product C_3H_6OOH of C_3H_8 leads to
315 the higher rate of production than CH_4. With C_3H_6 and C_2H_4, the reaction between the
316 formyl radical CHO and oxygen O_2 has the highest rate of production. The primary attack
317 on C_2H_4 is by addition of the O radical, and the primary products of this reaction are CH_3
318 and CHO radicals [34]. With respect to C_3H_6, it has been suggested that the O addition is
319 the dominant decay route through an intermediate complex, and the primary products of

this reaction are C_2H_5 and CHO radicals [34]. Thus, it may be suggested that the CHO radical production with C_3H_6 and C_2H_4 promotes the HO_2 production, although C_2H_5 and C_2H_4OOH also have non-negligible impacts on the rate of the HO_2 production.

4. Conclusions

To investigate the effects of EGR gas composition on the ignition delays in low temperature diesel combustion, the ignition delays were measured in a single-cylinder engine while introducing hydrocarbons and nitrogen oxides. The conclusions may be summarized as follows:

1. The ignition delay of the diesel combustion is decreased with introduced nitrogen oxide (NO) present in the intake, and its effect is more pronounced with higher intake temperatures.
2. The ignition promotion effects with nitrogen dioxide (NO_2) are more pronounced than those with NO.
3. Introducing carbon monoxide (CO) and hydrocarbons (CH_4, C_2H_4, C_3H_6 and C_3H_8) in the intake has little effect on the ignition delay.
4. Compared to feeding only NO, simultaneous feeding of NO and hydrocarbons achieves a shorter ignition delay of the diesel combustion. The hydrocarbons

producing more hydroperoxyl radicals (HO_2) tend to decrease the ignition delay as they enhance the $NO + HO_2 = NO_2 + OH$ reaction.

Small amounts of NO_x are recirculated under EGR conditions, and the effects on the ignition are notable with the recirculated hydrocarbons at higher intake temperatures.

References

[1] Kamimoto, T. and Bae, M.-H., High Combustion Temperature for the Reduction of Particulate in Diesel Engines, SAE Technical Paper, No.880423 (1988)

[2] Akihama, K., Takatori, Y., Inagaki, K., Sasaki, S. and Dean, A. M., Mechanism of the Smokeless Rich Diesel Combustion by Reducing Temperature, SAE Technical Paper, No.2001-01-0655 (2001)

[3] Ogawa, H., Li, T. and Miyamoto, N., Characteristics of Low Temperature and Low Oxygen Diesel Combustion with Ultra-high Exhaust Gas Recirculation, Int. J. Engine Research, Vol.8, Issue 4, pp.365-378 (2007)

[4] Kook, S., Bae, C., Miles, P. C., Choi, D. and Pickett, L. M., The Influence of Charge Dilution and Injection Timing on Low-Temperature Diesel Combustion and Emissions, SAE Technical Paper No.2005-01-3837 (2005)

[5] Li, T., Suzuki, M. and Ogawa, H., Characteristics of Smokeless Low Temperature Diesel Combustion in Various Fuel-Air Mixing and Expansion of Operating Load Range, SAE Technical Paper No.2009-01-1449 (2009)

[6] Kimura, S., Ogawa, H., Matsui, Y. and Enomoto, Y., An Experimental Analysis of Low-Temperature and Premixed Combustion for Simultaneous Reduction of NO_x and Particulate Emissions in Direct Injection Diesel Engines, Int. J. Engine Research, Vol.3, Issue 4, pp.249-259 (2002)

[7] Ming, J., Gingrich, E., Wang, H., Li, Y., Ghandhi, J. B. and Reitz, R. D., Effect of Combustion Regime on In-cylinder Heat Transfer in Internal Combustion Engines,

Int. J. Engine Research, Vol.17, Issue 3, pp.331-346 (2015)
[8] Li, T., Moriwaki, R. and Ogawa, H., Dependence of Premixed Low-temperature Diesel Combustion on Fuel Ignitability and Volatility, Int. J. Engine Research, Vol.13, Issue 1, pp.14-27 (2012)
[9] Zheng, Z., Yue, L., Liu, H., Zhu, Y., Zhong, X. and Yao, M., Effect of Two-stage Injection on Combustion and Emissions under High EGR Rate on a Diesel Engine by Fueling Blends of Diesel/Gasoline, Diesel/n-Butanol, Diesel/Gasoline/n-Butanol and Pure Diesel, Energy Conversion and Management, Vol.90, pp.1-11 (2015)
[10] Liu, H., Ma, S., Zhang, Z., Zheng, Z. and Yao, M., Study of the Control Strategies on Soot Reduction under Early-injection Conditions on a Diesel Engine, Fuel, Vol.139, pp.472-481 (2015)
[11] Shi, H., An, Y. and Johansson, B., Study of Fuel Octane Sensitivity Effects on Gasoline Partially Premixed Combustion Using Optical Diagnostics, SAE Technical Paper, No.2019-24-0025 (2019)
[12] Andree, A. and Pachernegg, S. J., Ignition Conditions in Diesel Engines, SAE Technical Paper No.690253 (1969)
[13] Ladommatos, N., Abdelhalim, S., Zhao, H. and Hu, Z., Effects of EGR on Heat Release in Diesel Combustion, SAE Technical Paper No.980184 (1998)
[14] Rieß, S., Vogel, T. and Wensing, M., Influence of Exhaust Gas Recirculation on Ignition and Combustion of Diesel Fuel under Engine Conditions Investigated by Chemical Luminescence, 13th Triennial International Conference on Liquid Atomization and Spray Systems, Tainan (2015)
[15] Ogawa, H., Morita, A., Futagami, K. and Shibata, G., Ignition Delays in Diesel Combustion and Intake Gas Conditions, Int. J. Engine Research, Vol.19, Issue 8, pp.805-812 (2018)
[16] Kawabata, Y., Sakonji, T. and Amano, T., The Effect of NO_x on Knock in Spark-Ignition Engines, SAE Technical Paper No.1999-01-0572 (1999)
[17] Sjöberg, M., Dec, J. E. and Hwang, W., Thermodynamic and Chemical Effects of EGR and Its Constituents on HCCI Autoignition, SAE Technical Paper No.2007-01-0207 (2007)
[18] Kawasaki, K., Kubo, S., Yamane, K. and Kondo, C., The Effect of the Induction of Nitrogen Oxides on Natural Gas HCCI Combustion, SAE Technical Paper No.2014-01-2697 (2014)
[19] Hori, M., Matsunaga, N., Marinov, N., Pitz, W. and Westbrook, C., An Experimental and Kinetic Calculation of the Promotion Effect of Hydrocarbons on the NO-NO_2 Conversion in a Flow Reactor, Twenty-Seventh Symposium on Combustion, pp.389-

396 (1998)
[20] Anderlohr, J. M., Bounaceur, R., Cruz, A. P. D. and Battin-Leclerc, F., Modeling of Autoignition and NO Sensitization for the Oxidation of IC Engine Surrogate Fuels, Combustion and Flame, 156, pp.505-521 (2009)
[21] Kobashi, Y., Yuze, S., Ogawa, H., Shibata, G., Kato, S., Nishijima, Y., Kondo, W., Morishima, S., Kawakita, S., Fujino, T. and Ito, T., Auto-ignition Characteristics of Gasoline Sprays with Two-stage Injection in CI Engines, COMODIA 2017 (2017)
[22] Iida, N., Nakamura, M. and Ohashi, H., Study of Diesel Spray Combustion in an Ambient Gas Containing Hydrocarbon Using a Rapid Compression Machine, SAE Technical Paper No.970899 (1997)
[23] Nitta, Y., Niki, Y., Hirata, K. and Yamasaki, Y., Effects of the Combustion Characteristics of Diesel Engine by the Intake of Exhaust Gas from Gas Engine, Journal of the JIME, Vol.53, No.3, pp.119-124 (2018)
[24] Asai, G., Tokuoka, Y., Bayer, T., Ishiguro, S., Shibata, G., Ogawa, H., Kobashi, Y. and Watanabe, Y., A Study of a Lean Homogeneous Combustion Engine System with a Fuel Reformer Cylinder, SAE Technical Paper No.2019-01-2177 (2019)
[25] Asai, G., A Study of Gas-Diesel Dual Fuel Combustion for Higher Thermal Efficiency and Lower Emissions, YANMAR Technical Review, (2019) https://www.yanmar.com/br/technology/technical_review/2019/1001_6.html
[26] CHEMKIN 15151, ANSYS Reaction Design: San Diego (2016)
[27] Atkinson, R., Baulch, D. L., Cox, R. A., Crowley, J. N., Hampson, R. F., Hynes, R. G., Jenkin, M. E., Rossi, M. J. and Troe, J., Evaluated Kinetic and Photochemical Data for Atmospheric Chemistry: Volume I – Gas Phase Reactions of O_x, HO_x, NO_x and So_x Species, Atoms. Chem. Phys., 4, pp.1461-1738 (2004)
[28] Liu, H., Cui, Y., Chen, B., Kyritsis, D. C., Tang, Q., Feng, L., Wang, Y., Li, Z., Geng, C. and Yao, M., Effects of Flame Temperature on PAHs and Soot Evolution in Partially Premixed and Diffusion Flames of a Diesel Surrogate, Energy & Fuels, Vol.33, pp.11821-11829 (2019)
[29] Geng, C., Liu, H., Cui, Y., Yang, Z., Fang, X., Feng, L. and Yao, M., Study on Single-fuel Reactivity Controlled Compression Ignition Combustion through Low Temperature Reforming, Combustion and Flame, Vol.199, pp.429-440 (2019)
[30] Gokulakrishnan, P., Fuller, C. C., Klassen, M. S., Joklik, R. G., Kochar, Y. N., Vaden, S. N., Lieuwen, T. C. and Seitzman, J. M., Experiments and Modeling of Propane Combustion with Validation, Combustion and Flame, Vol.161, Issue 8, pp.2038-2053 (2014)
[31] Gokulakrishnan, P., Fuller, C. C. and Klassen, M. S., Experimental and Modeling

437 Study of C_1-C_3 Hydrocarbon Ignition in the Presence of Nitric Oxide, J. Eng. Gas
438 Turbines Power, Vol.140, Issue 4, pp.041509-1-041509-9 (2018)
439 [32] Zheng, Z. and Lv, Z., A New Skeletal Chemical Kinetic Model of Gasoline Surrogate
440 Fuel with Nitric Oxide in HCCI Combustion, Applied Energy, Vol.147, pp.59-66
441 (2015)
442 [33] Naruke, M., Yoshida, S., Wachi, Y., Tanaka, K. and Konno, M., The Effect of EGR
443 on Ignition Characteristics of Gasoline Under Lean Burn Conditions, 11th Asia-
444 Pacific Conference on Combustion (2017)
445 [34] Glassman, I., *Combustion – Third Edition*, Academic Press (1996)
446

Table 1 Specifications of the test engine

Type of engine	4TNV98T (Yanmar)
Bore x stroke [mm]	98 x 110
Displacement volume [cm^3]	830
Compression ratio [-]	17.6
Type of injector	G4S (DENSO)
Nozzle hole diameter [mm]	0.125
Included spray angle [º]	155
Number of nozzles	8

Table 2 Gaseous species determined with the FTIR spectrometer

CO	CO_2	NO	NO_2	N_2O
H_2O	NH_3	SO_2	HCHO	CH_3CHO
CH_3OH	C_3H_6O	MTBE	HCOOH	CH_4
C_2H_4	C_2H_6	C_3H_6	1,3-C_4H_6	iso-C_4H_8
C_6H_6	C_7H_8			

Table 3 Experimental conditions

Engine rotation speed [rpm]	1000
IMEP [MPa]	0.25
Intake air	Naturally aspirated
Intake air temperature, T_{in} [ºC]	100, 125, 150
Injection pressure [MPa]	86
Injection quantity [mm^3/cycle]	20
Intake oxygen concentration [%]	7
Intake NO_x concentration [ppm]	0 - 1200

Table 4 Fractions of NO and NO_2 in the intake gas, measured with the FTIR spectrometer

T_{in} = 100ºC		T_{in} = 125ºC		T_{in} = 150ºC	
NO [ppm]	NO_2 [ppm]	NO [ppm]	NO_2 [ppm]	NO [ppm]	NO_2 [ppm]
110	120	50	60	0	0
230	180	110	120	0	15
320	260	180	130	60	70
410	350	230	170	-	-

Table 5 Intake gas composition as the experimental variable

	O_2 [%]	N_2	CO [%]	NO [ppm]	CH_4 [ppmC]	C_2H_4 [ppmC]	C_3H_6 [ppmC]	C_3H_8 [ppmC]
CO	11	balance	0 – 4	-	-	-	-	-
NO			-	0 – 470	-	-	-	-
$NO+CH_4$				0 – 200	10000	-	-	-
$NO+C_2H_4$				0 – 200	5000	5000	-	-
$NO+C_3H_6$					5000	-	5000	-
$NO+C_3H_8$					5000	-	-	5000

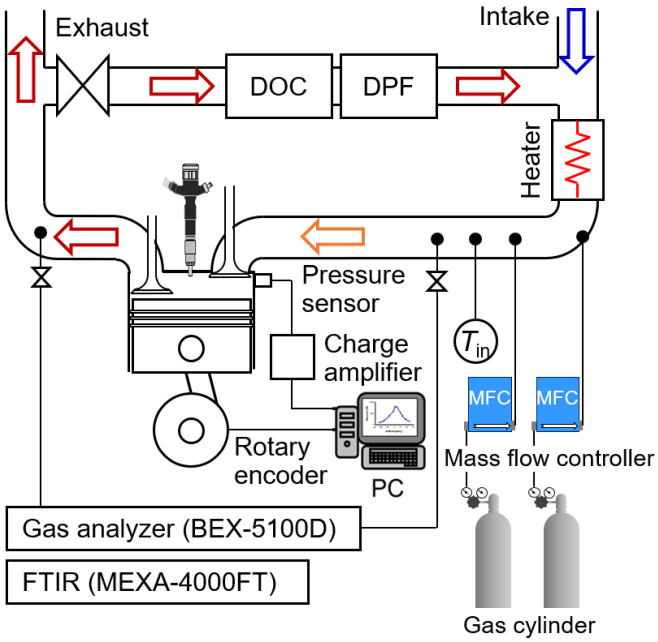

Fig.1 Outline of the experimental setup

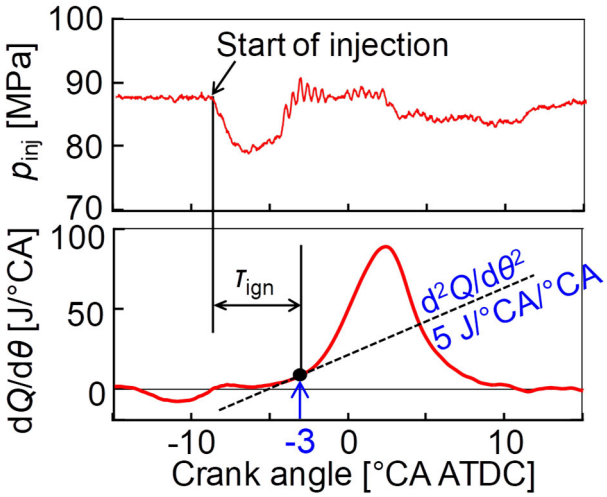

Fig.2 Definition of the ignition set at -3°CA ATDC and the ignition delay τ_{ign}

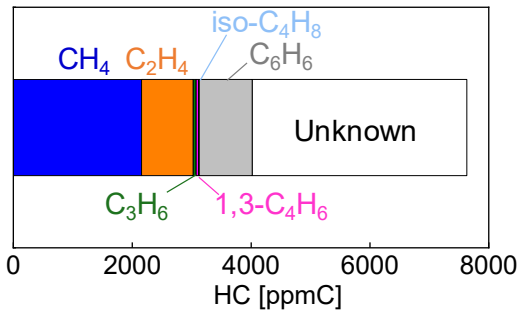

Fig.3 Measured intake hydrocarbon species (T_{in} = 125°C)

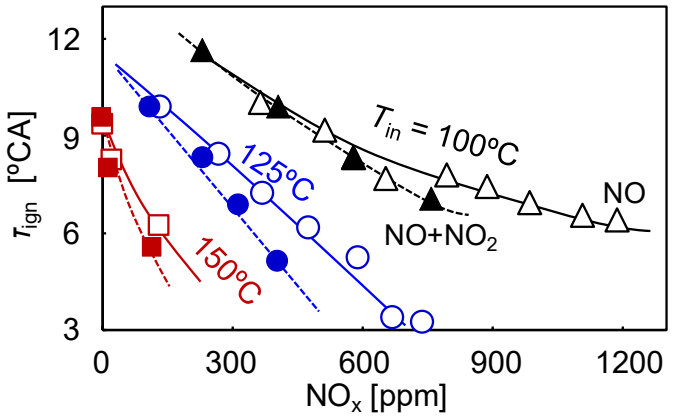

Fig.4 Effect of NO and NO_2 introduced in the intake gas vs the ignition delay τ_{ign} (w/EGR, open symbols: NO addition, closed symbols: NO + NO_2 addition)

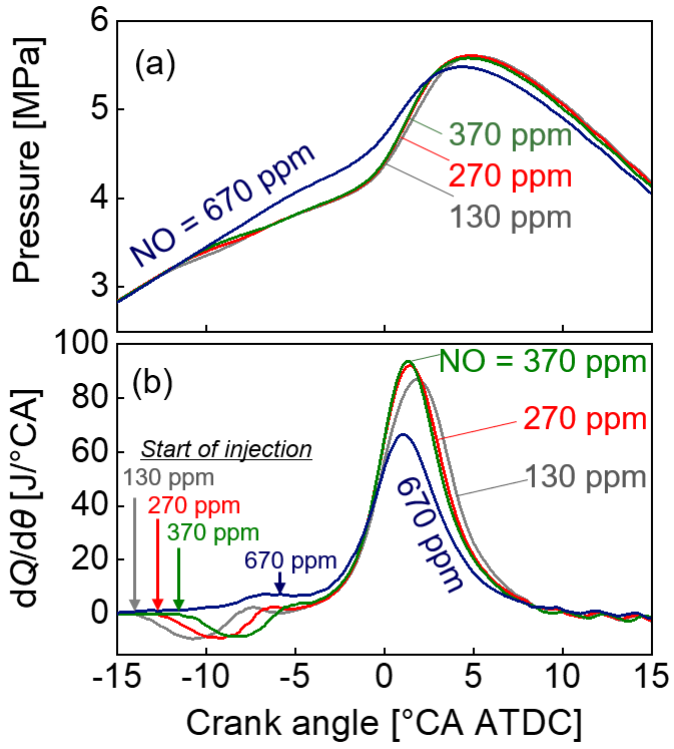

Fig.5 Profiles of in-cylinder pressure and heat release rate dQ/dθ, changed with the NO concentration (T_{in} = 125°C, w/EGR)

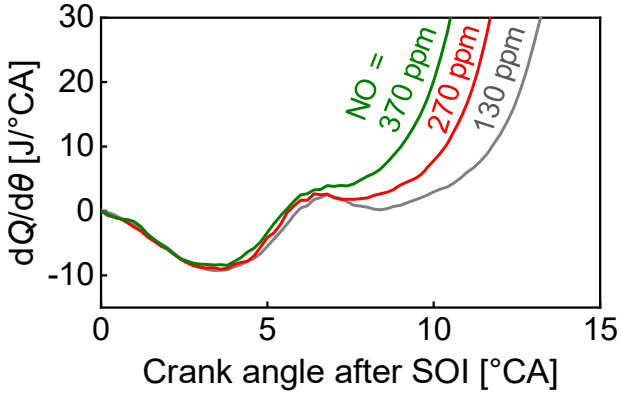

Fig.6 Profiles of heat release rate dQ/dθ, arranged against the crank angle after the start of injection (SOI) (T_{in} = 125°C, w/EGR)

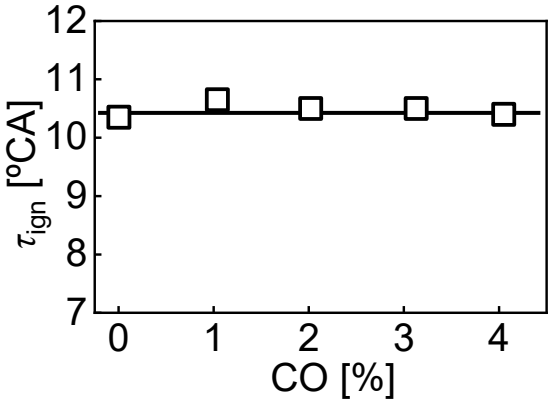

Fig.7 Ignition delays τ_{ign} vs changes in the intake CO concentration (T_{in} = 125°C, NO = 0 ppm)

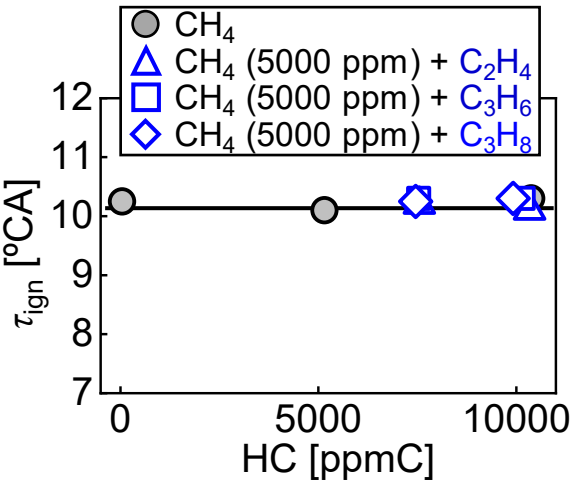

Fig.8 Ignition delays τ_{ign} vs changes of the intake hydrocarbon species and concentrations (T_{in} = 125°C, NO = 0 ppm)

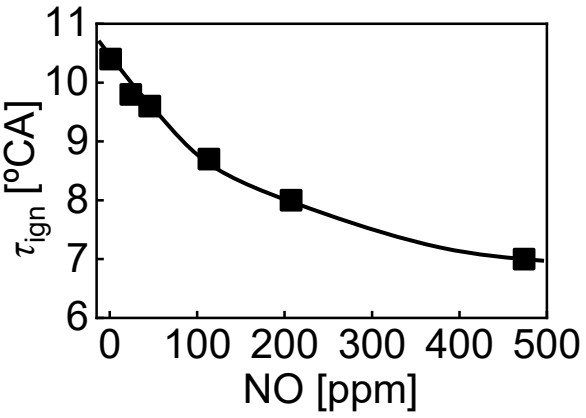

Fig.9 Ignition delays τ_{ign} vs changes of the intake NO concentration (T_{in} = 125°C, HC = 0 ppmC)

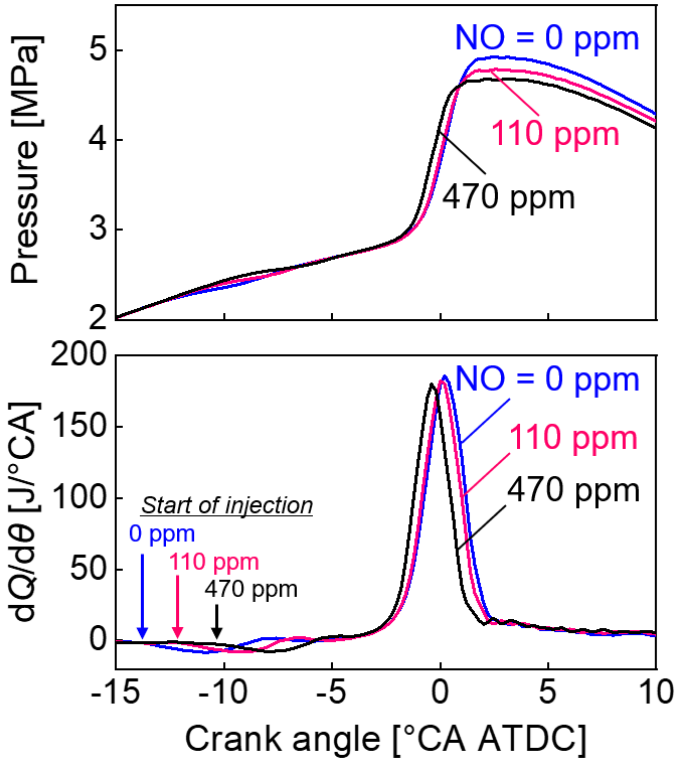

Fig.10 Profiles of the in-cylinder pressure and heat release rate dQ/dθ, changed with the NO concentration (T_{in} = 125°C, HC = 0 ppmC)

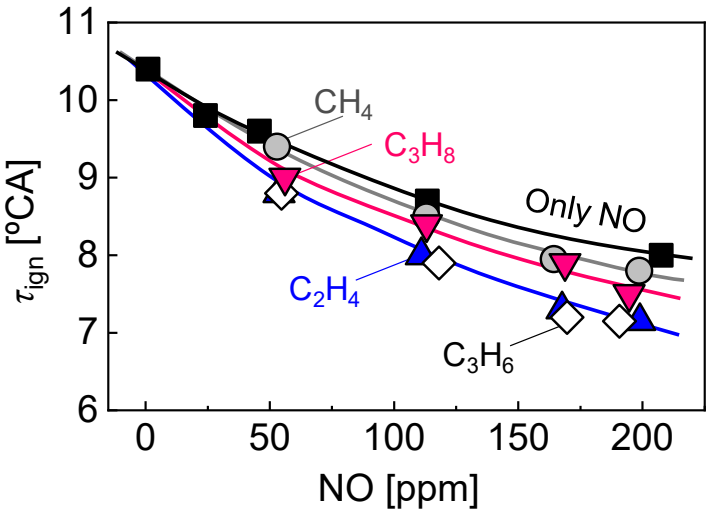

Fig.11 Effects of hydrocarbon species and NO concentration on the ignition delay τ_{ign} (T_{in} = 125°C, HC = 10000 ppmC)

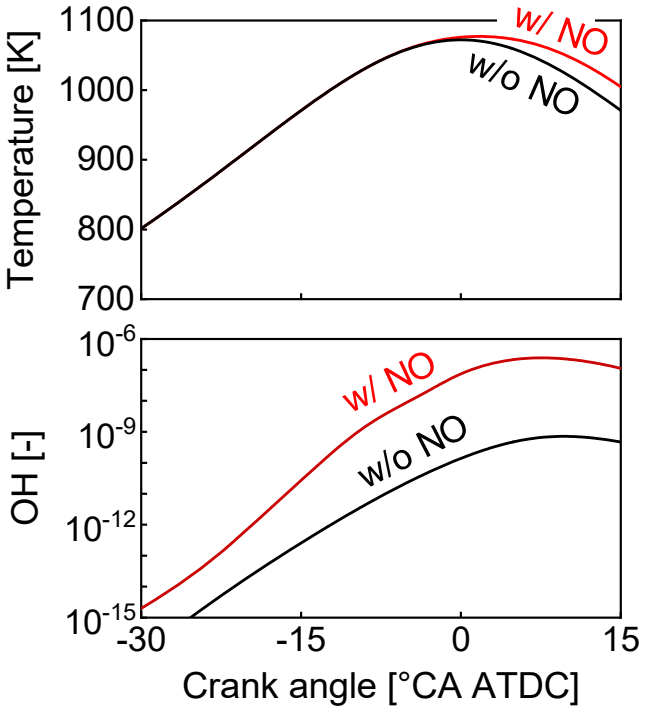

Fig.12 Calculated profiles of the in-cylinder mean temperature and OH concentration (CH_4 = 5000 ppmC, C_2H_4 = 5000 ppmC, NO = 100 ppm)

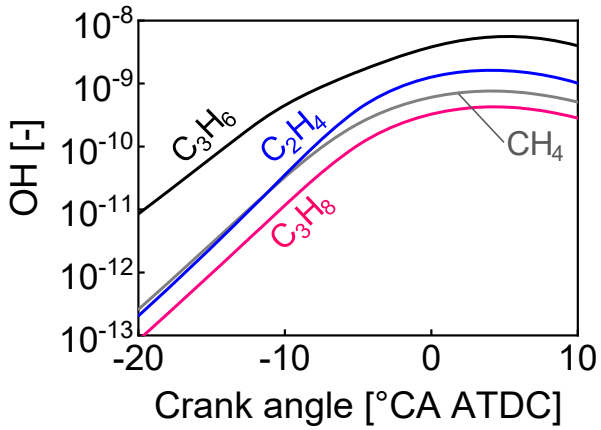

Fig.13 Plot of calculated OH concentrations for the tested hydrocarbon species (HC = 10000 ppmC, NO = 100 ppm)

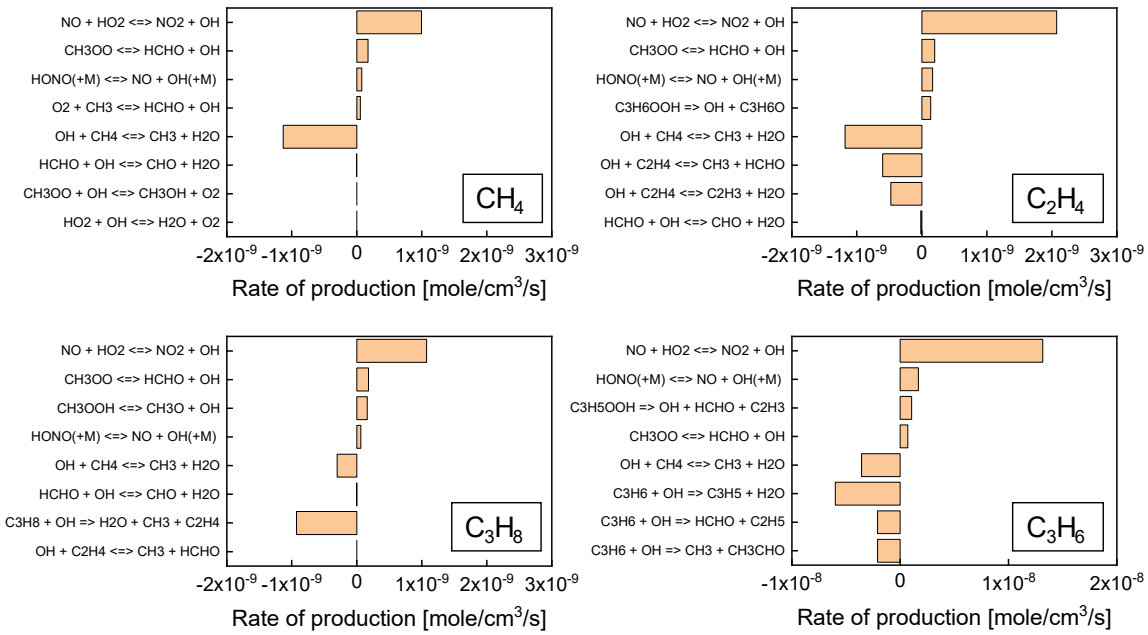

Fig.14 Major OH production rates and their chemical equations for the tested hydrocarbon species (HC = 10000 ppmC, NO = 100 ppm)

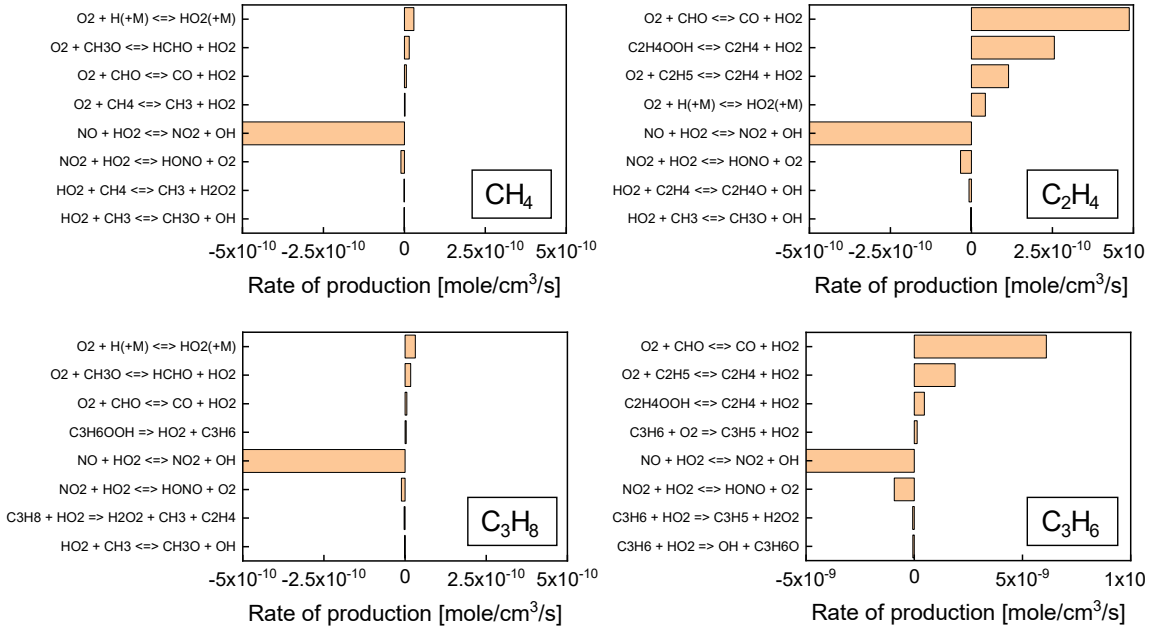

Fig.15 Major HO_2 production rates and their chemical equations for the tested hydrocarbon species (HC = 10000 ppmC, NO = 100 ppm)